Highly spatial resolved measurements of turbulent boundary layers by a laser Doppler velocity profile sensor

[1)]Büttner, L., [1)]Shirai, K., [1)]Razik, T., [1)]Czarske, J.,
[2)]Müller, H., [2)]Dopheide, D., [3)]Becker, S., [3)]Lienhart, H., [3)]Durst, F.

[1)] Laser Zentrum Hannover e.V. (LZH) , Grp. Laser Metrology
Hollerithallee 8, D-30419 Hannover, Germany
E-mail: cz@lzh.de, Internet: www.lzh.de

[2)] Physikalisch-Technische Bundesanstalt (PTB), Department for Gas Flow
Bundesallee 100, D-38116 Braunschweig, Germany

[3)] Friedrich-Alexander-Universität Erlangen-Nürnberg, Lehrstuhl für Strömungsmechanik (LSTM)
Cauerstr. 4, D-91058 Erlangen, Germany

ABSTRACT

We report about the application of a novel laser Doppler velocity profile sensor for spatially high resolved velocity measurements. The profile sensor employs a two-wavelength technique, which generates a measurement volume with convergent and divergent fringes (Fig. 1). The evaluation of the ratio of the resulting two Doppler frequencies yields the position inside the measurement volume with up to micrometer accuracy. We report about the application of the sensor for the measurement of laminar and turbulent boundary layers and for the determination of the wall shear stress. A good agreement between the measured velocity profiles and hot-wire measurements as well as the theory is obtained. The sensor offers the potential for the high resolved measurement of turbulent shear flows as well as of flows in micro-fluidics channels.

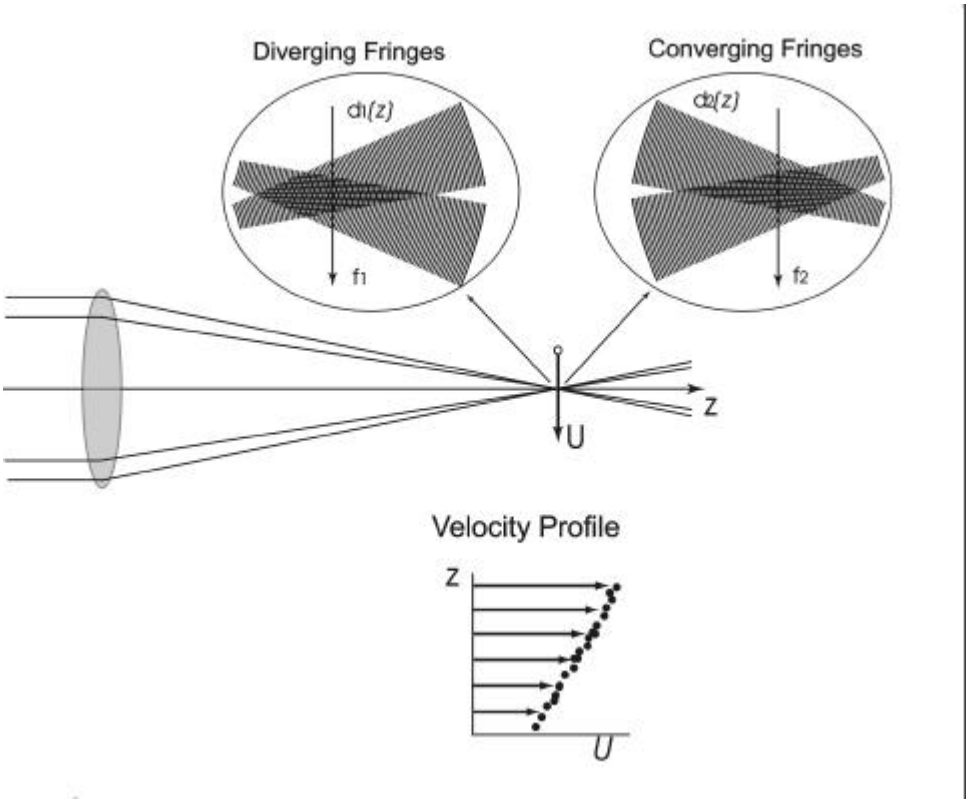

Fig.1: The principle of the laser Doppler velocity profile sensor. Top: Generation of the bichromatic measurement volume consisting of converging and diverging fringes. Bottom: Spatial resolved velocity measurement inside the measurement volume.

1. INTRODUCTION

Spatially high resolved velocity measurements are of great importance in fluid mechanics studies and applications. In a turbulent flow the smallest scale of vortices becomes smaller and the thickness of a boundary layer becomes thinner with increasing flow Reynolds number. The Reynolds number of flows can be at the order of 10^6 and the smallest vortex scale can be in the micro meter range [Fischer et al. 2001]. One of the measurement demands with high spatial resolution is the velocity measurement close to the wall in turbulent flows. Since the velocity becomes zero at the wall due to the non-slip condition, there is a steep velocity gradient close to the wall. In order to resolve structures in such a flow a velocity measurement with micron resolution is desired. A velocity measurement with high spatial resolution is also important for the microfluidics flow applications. Microfluidics devices utilise flow channels with the dimension of down to typically 10 µm. In order to know the structure inside such a flow the spatial resolution with micrometer range is necessary. In microfluidics research, particle-image velocimetry (PIV) or particle-tracking velocimetry (PTV) with micrometer resolution have been mainly used for obtaining sub-micrometer scales in a measurement field [Meinhart et al. 1999, 2000, Sato et al. 2003].

For a high spatial resolved measurement, a non-intrusive measurement technique should be applied not to disturb the flow with a probe. Laser Doppler anemometry (LDA) is a well-established technique for local velocity measurements with relatively high precision [Albrecht et al. 2002]. Usually, a differential Doppler technique is applied, which is based on a Mach-Zehnder interferometer. Two coherent laser beams generate an interference fringe system, which defines the measurement volume. The size of measurement volume determines the spatial resolution of the velocity measurement. But a conventional LDA is not enough for getting high spatial resolution due to the spatial averaging effect inside the measurement volume. Although a correction method based on the near-wall velocity-distribution has been proposed to decrease the spatial average effect [Durst et al. 1996, 1998], it cannot be applied for a flow field with arbitrary velocity distribution. A resolution of about 20 µm can be achieved by strong focusing of the laser beams [Nijhof et al. 1993, Tieu et al. 1995] or by the use of beam stops in the receiving optics [Mazumder et al. 1981]. However, a further increase in the spatial resolution is critical in general, since the accompanying wave-front distortion causes the non-uniformity of fringe spacing inside the measurement volume [Miles 1996] and the low number of fringes degrades the accuracy of the Doppler frequency estimation. An alternative way is to decrease the length of the measurement area without decreasing the number of fringes by using a low coherent light source together with a multi-mode fiber [Büttner and Czarske 2001].

To overcome these limitations a laser Doppler velocity profile sensor has been proposed [Czarske 2001, Czarske et al. 2002, Büttner and Czarske 2003]. It uses two different interference fringe systems, which are superposed to create a measurement volume. The position as well as the velocity of a tracer in the measurement volume can be determined by the measured Doppler frequencies and a calibration function. As the sensor does not assume any velocity distribution, it can be applied for a flow with arbitrary velocity profile. Besides, in contrast to the micro-PIV /PTV techniques the spatial resolution of the velocity profile sensor is not based on imaging whose spatial resolution is limited by diffraction [Meinhart and Wereley 2003], that of the profile sensor can be potentially achieved down to sub-micrometer scale. Since the profile sensor is an extension of the conventional LDA, it can have a long working distance, which is suitable for most of flow-measurement applications.

In this study we show the applicability of the LDA velocity profile sensor to turbulent flow measurements. First the working principle will be shown. Then the measurement accuracy will be estimated by theory and experiment. The sensor was applied for the measurement in free stream, followed by the measurements in laminar and turbulent boundary layers. The wall shear stress was estimated by the measured velocity profile close to the wall.

2. LDA VELOCITY PFOFILE SENSOR

2.1 Principle

The velocity profile sensor is an extension of the known laser Doppler technique. The profile sensor utilises two interference fringe systems: one is diverging and the other is converging, which are generated by two laser wavelengths (Fig. 2). Therefore it enables the velocity measurement with spatial resolution inside the measurement volume [Czarske et al. 2002].

The Doppler shift frequency caused by a moving scattering particle is expressed as [Albrecht et al. 2002]

$$f_D = \frac{U}{d}, \tag{1}$$

where U is the velocity of the particle perpendicular to the bisector of the incident beams and d is the fringe spacing. Usually the fringes in the measurement volume are considered to be parallel and equally distanced. However, any LDA fringe system generated by Gaussian beams has non-uniform fringe spacing both in optical axis (bisector of the beams) and the direction perpendicular to the optical axis, due to the wavefront curvature of laser beam [Miles 1996]. The non-uniformity becomes smallest when the beam waists are adjusted so that they coincide at the crossing point of the beams. The fringe non-uniformity perpendicular to the optical axis determines the minimum turbulent intensity measured by the system. The laser Doppler velocity profile sensor utilises the non-uniformity of fringe spacing along the optical axis. When the beam waists are located before or behind the beam crossing point, the fringe spacing becomes a monotonic increasing or decreasing function in the optical axis, respectively:

$$d_i = d_i(z), \tag{2}$$

where i=1, 2 and z is the position along the optical axis (Fig. 2). The measured Doppler frequencies for each wavelength becomes also the function of the position,

$$f_i = f_i(z). \tag{3}$$

The quotient of the measured two Doppler frequencies should be a monotonic function of the position of a tracer-particle path inside the measurement volume,

$$q(z) = \frac{f_2(z)}{f_1(z)} = \frac{U(z)/d_2(z)}{U(z)/d_1(z)} = \frac{d_1(z)}{d_2(z)}. \tag{4}$$

As the quotient is independent of the velocity, the position z can be determined by the inverse function of the quotient,

$$z = z(q), \tag{5}$$

and the fringe spacings are determined from the tracer particle position. Then the velocity at the position is calculated by the measured Doppler frequency and the calculated fringe spacing,

$$U(z) = f_1(U,z)\cdot d_1(z) = f_2(U,z)\cdot d_2(z). \tag{6}$$

Therefore, the position of tracer particle as well as the velocity can be precisely measured, if the quotient curve is known.

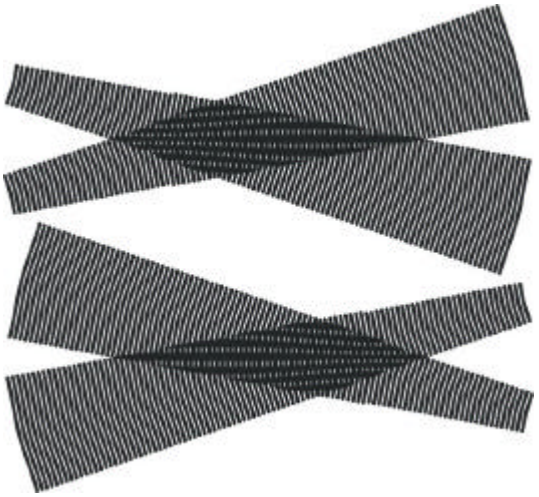

Fig. 2: Generation of two (overlapping) interference fringe systems by means of two laser wavelengths, one with divergent, the other with convergent fringes.

2.2 Set up of the sensor system

The set up of the profile sensor is shown in Fig. 3. The beams from two laser diodes (λ_1 = 658 nm, λ_2 = 785 nm) were collimated with aspherical lenses and collinearly combined by a dichroic mirror. The combined beam is divided into two beams with prism beam splitter and the beams enter the telescope. Then the beams are focused by the lens with focal length of 300mm to create the measurement volume at the intersection point. The laser diodes can be adjusted independently to generate the convergent and divergent fringe systems. The scattered light was collected with forward-scattering mode and it was guided through the multi-mode fibre. The guided light was divided into the two wavelength components (λ_1, λ_2) by a dichroic mirror and was converted to electric signals with photo-detectors. The analogue-to-digital conversion for two channels was accomplished with 12 bit data acquisition PC card. The power spectrum for each channel was calculated by FFT technique with zero-padding and the frequency peak was detected by 7-point linear interpolation. These calculations were software-implemented by a LabVIEW program.

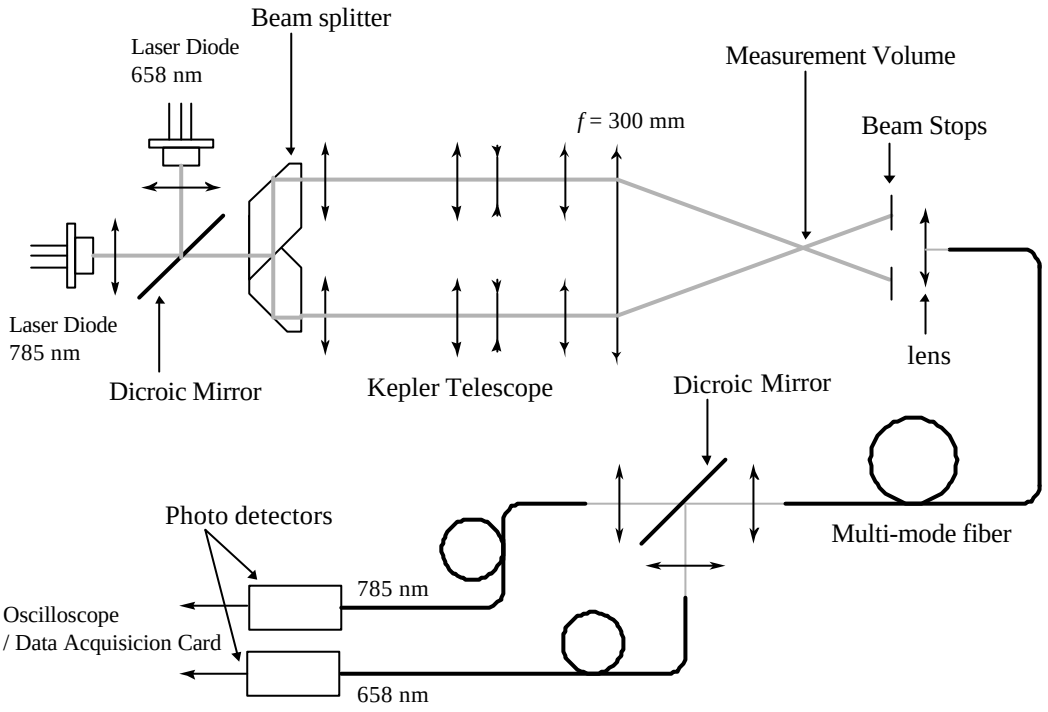

Fig.3: Arrangement of the profile sensor with heterodyne technique.

2.3 Calibration of the profile sensor

The sensor was adjusted to obtain a high spatial resolution inside the measurement volume. The position of each laser diode was adjusted carefully so that one of the fringe becomes diverging and the other becomes converging. The details about the optical adjustments were discussed by Büttner [Büttner 2004]. The results of the beam adjustment are shown in Fig. 4, 5, 6. Fig. 4 shows the amplitude variation of the power spectrum along the *z*-axis for each wavelength beams. From Fig. 4 the measurement volume can be defined and it ranges for 750 µm in the *z*-axis. It can be seen that the centre of the measurement volume is not identical for the both wavelength beams. This is caused by the remaining chromatic aberration effect. Fig. 5 is the variation of the fringe-spacing for the two wavelengths and Fig. 6 is the calibration curve, with which the *z*-position of the particle is determined.

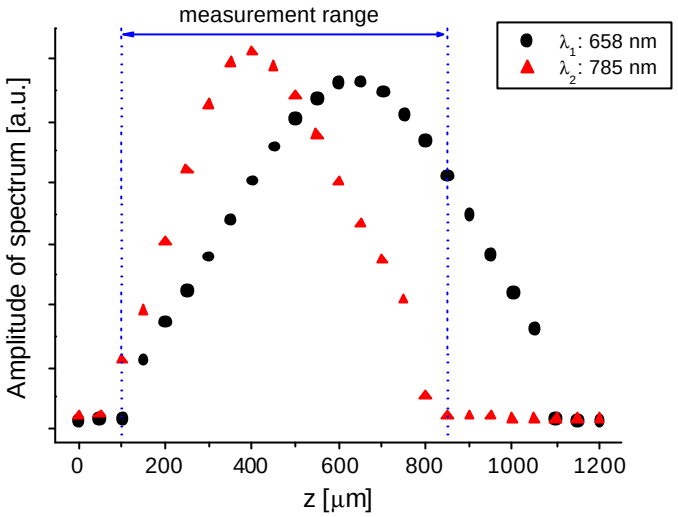

Fig.4: Amplitude variation of the power spectrum along z-axis.

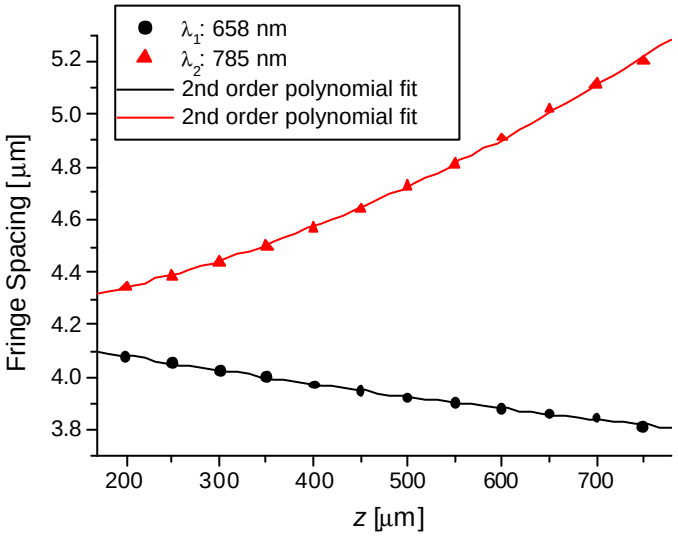

Fig.5: Fringe-spacing variation along the z-axis.

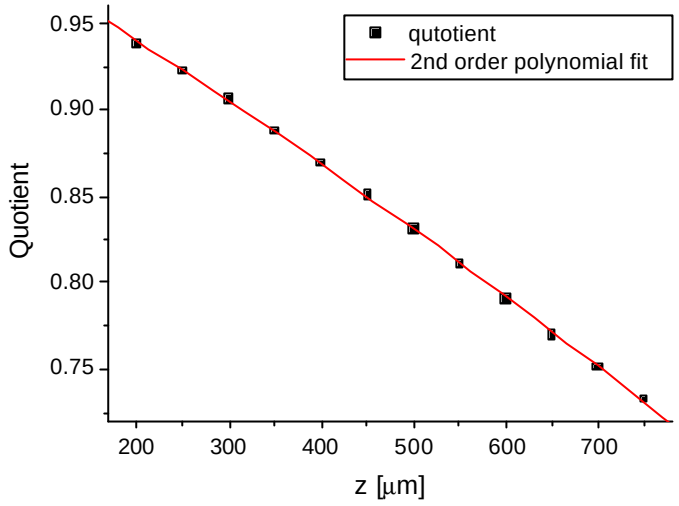

Fig.6: Calibration curve for determining the z-position from the measured Doppler frequency (the variation of the quotient of the fringe-spacing.

3. INVESTIGATION ON THE MEASUREMENT ACCURACY

The spatial resolution of the profile sensor is determined by the slope of the calibration curve and the frequency estimation accuracy [Czarske et al. 2002]. If the standard deviation of the frequency estimation accuracy is the same for both wavelengths, the spatial resolution can be approximated by

$$\Delta z \approx \sqrt{2}\left|\frac{\partial z}{\partial q}\right|\frac{\Delta f}{f}, \tag{7}$$

where q is the quotient and Df is the standard deviation of the frequency. Then the relative velocity measurement accuracy can be approximated as

$$\frac{\Delta U}{U} \approx \sqrt{\frac{3}{2}} \cdot \frac{\Delta f}{f}. \tag{8}$$

From the above equations the spatial resolution and the relative velocity measurement accuracy can be theoretically estimated. With the slope of the calibration curve and the typical estimation accuracy of the Doppler frequency of about $Df/f \sim 10^{-4}$, the spatial resolution of 0.4 µm and the relative velocity measurement accuracy of $DU/U \sim 1.2\times10^{-4}$ can be expected.

The measurement accuracies of z-position and velocity were experimentally investigated with a scattering wire. A tungsten wire (diameter: 4 µm) was attached on a rotating disc to simulate a tracer particle in a fluid flow. The resulting measurement accuracies are shown in Fig. 7 for two different rotation speed of the chopper. The averaged measurement accuracy of z-position was Δz = 3.0 µm and Δz = 7.7 µm for $V_{chopper}$=1.07 m/s and $V_{chopper}$=3.20 m/s Hz, respectively. The relative measurement accuracy of the velocity was $DU/U \sim 8.4\times10^{-4}$ and $DU/U \sim 2.1\times10^{-3}$ for $f_{chopper}$ = 50 Hz and $f_{chopper}$ = 150 Hz, respectively. The values of the spatial resolution investigated by the experiment were one order of magnitude larger than the predicted value. The reason for the lower spatial resolution compared to the prediction can be attributed to the distortion of the plate itself, since the scattering object is not expected to be stable with micrometer accuracy when operated. But the relative measurement accuracy of the velocity agrees well to the predicted value. This shows the sensor has a very low systematic measurement error.

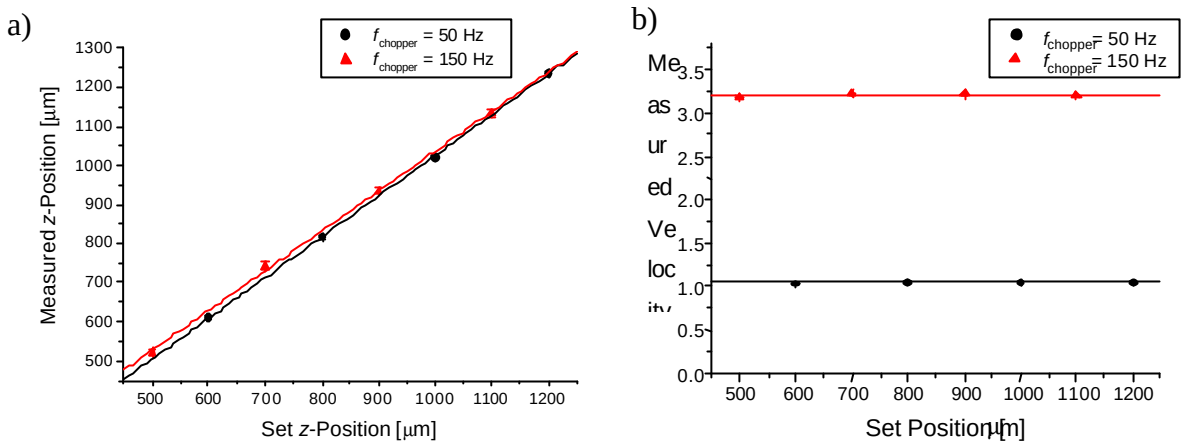

Fig.7: Experimental measurement accuracy with different chopper velocity and locations: a) z-position (lines are linear fit), b) velocity (lines are linear fit).

4. WIND TUNNEL MEASUREMENTS

4.1 Free stream measurements

First the free stream measurement was conducted in the Eiffel-type wind tunnel of the Physikalisch-Technische Bundesanstalt (PTB). A water-glycerine suspension with particles of about 1 µm diameter was used for seeding the flow. The measurement volume was placed near the centre of the test section of the wind tunnel. For the fluid flow measurements, the LabView program was provided with a validation procedure to avoid outlier data. Signals were validated only when the signal-to-noise ratio of both channels exceeded a certain threshold (coincidence validation) and when the estimated quotient of the Doppler frequencies was within the range defined by Fig. 6. For different rotating speeds of the wind tunnel fan a series of burst signals were recorded and both the mean values and the standard deviations were computed. Fig. 8 shows the turbulence intensity in dependence of the free-stream velocity. The turbulent intensity was almost constant around 0.6 %, though a slightly higher value can be seen as for low velocities.

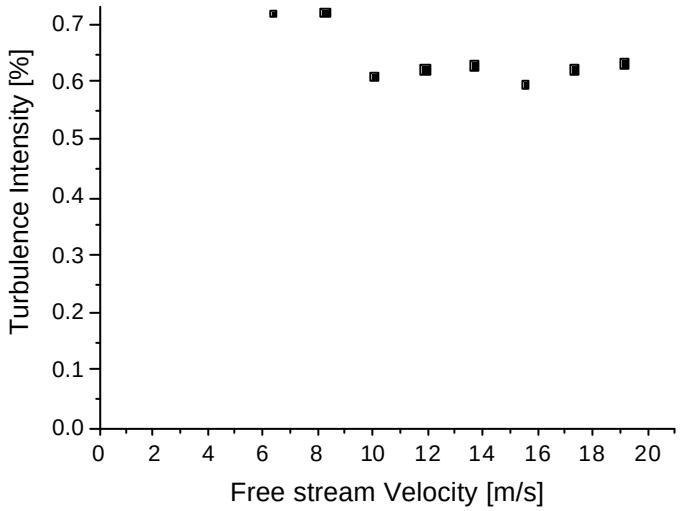

Fig.8: Free-stream turbulence intensity of the Eiffel-type wind tunnel in the PTB for different free stream velocities.

4.2 Boundary layer measurement

Then measurements were conducted in a closed-loop wind tunnel with open test section of the Göttingen-type at the LSTM. A glass plate with a NACA-profile at the leading edge was placed in the centre of the test section. DEHS (diethylhexylsebacate)- droplets with 2.5 µm mean diameter acted as scattering particles.
The measured velocity profile in a laminar boundary layer is shown in Fig. 9. Due to the thick boundary layer the measurement was conducted with traversing the measurement volume five times inside the boundary layer. Each of different symbols in the graph indicates different measurement range with a little overlap between the individual ranges. The measured profile is well-matched with that of the time-averaged data taken by a hot-wire anemometer together with the profile sensor. This indicates that sensor has a capability of measuring the velocity distribution inside the boundary layer.

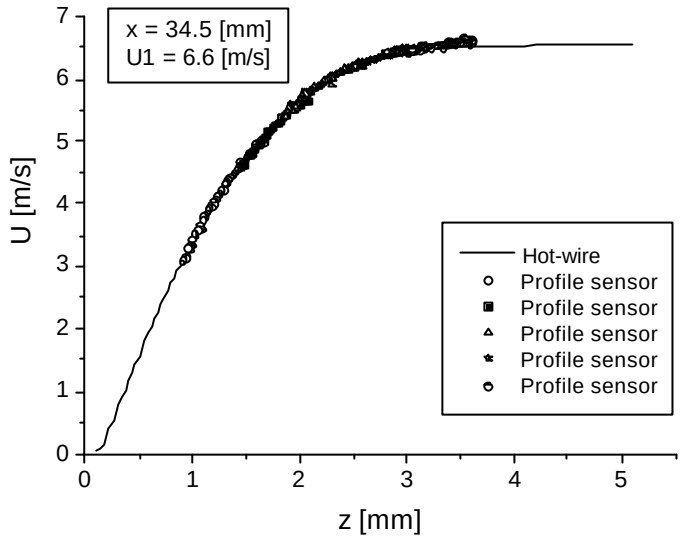

Fig. 9: The measurement result of a laminar boundary layer at a flat glass plate. The results are shown together with the hot-wire anemometer measurement. Sensor was traversed five times and each of the symbols indicates different measurement range.

The velocity profile in the vicinity of the wall can be used to determine the wall shear stress, which is an important measure for the skin friction of objects in fluid flows. The wall shear stress was calculated by fitting the measurement close to the wall (Fig. 10). The definition of the wall shear stress is [Schlichting and Gersten 2000]

$$t_w = m \left. \frac{dU}{dz} \right|_{z_{Wall}} \tag{9}$$

where z is the axis normal to the wall. This definition can be used to derive the wall shear stress from the gradient of the measured velocity profile close to the wall. For laminar flows the wall shear stress can be derived analytically from the Blasius theory [Schlichting and Gersten 2000]:

$$t(x, v_\infty) = 0{,}332 \cdot m \sqrt{\frac{U_\infty^3}{2nx}} \tag{10}$$

where µ means the dynamic viscosity, ν the kinematic viscosity of air, x the position from the leading edge of the glass plate and U_∞ the free stream velocity of the flow.
Fig. 11 shows the wall shear stress which was experimentally determined by means of the measured velocity profiles and Eq. (9) in comparison with the theoretical curve calculated by Eqn. (10). They show good agreement and it indicates that the profile sensor can be used for measuring the wall shear stress without mechanical traversing.

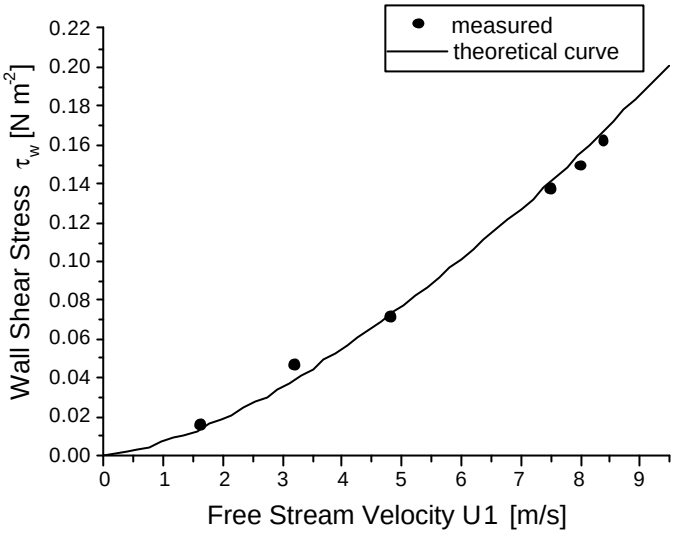

Fig. 10: Measured wall shear stress together with theoretical curve.

In order to obtain a turbulent boundary layer an obstacle (wire of about 1 mm diameter) was spanned upstream across the glass plate.
From each evaluated burst signal the program provides a data pair of velocity und position. Data are therefore continuously distributed with respect to the position. In order to make a spatial dis tributed statistics the data are attached to certain intervalls (slots), in which the velocity is considered constantly. For each slot the mean velocity and the standard deviation were calculated. Fig. 11 shows a fraction of the turbulent boundary layer in slot representation. The slot length was chosen to 10 µm. Fig. 11, top, shows the mean velocity and the standard deviation, in Fig. 11, bottom, the number of burst signals per slot is displayed.

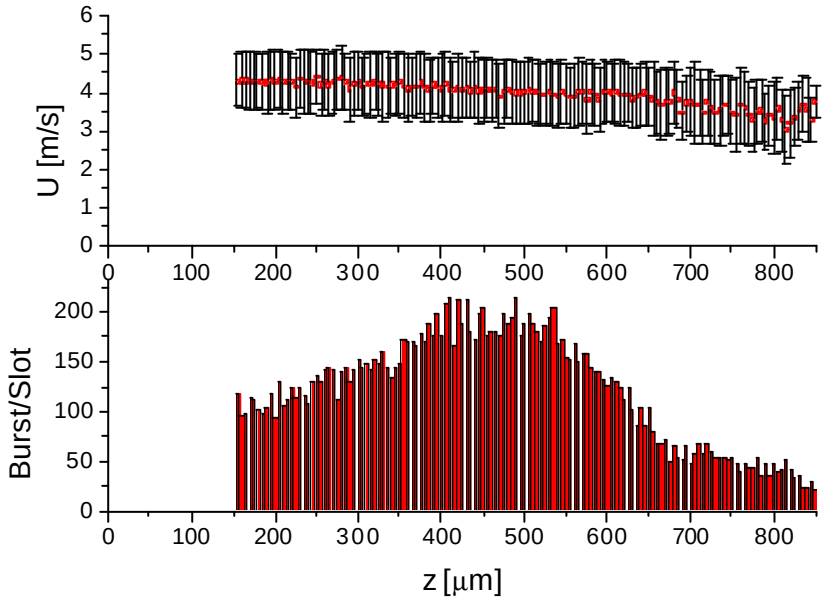

Fig.11: The measurement results in a turbulent boundary layer plate (top: raw measurement data, bottom: histogram of the number of bursts with the slot of 10 µm interval).

Fig. 12 shows a comparison between a laminar and turbulent boundary layer (with and without the obstacle). A significant change in the velocity profile and an overall increase of the turbulence intensity could be observed. The turbulence intensity increased from 0.35 % in the undisturbed flow (remaining turbulence intensity of the wind tunnel) to 12 % in the disturbed flow.

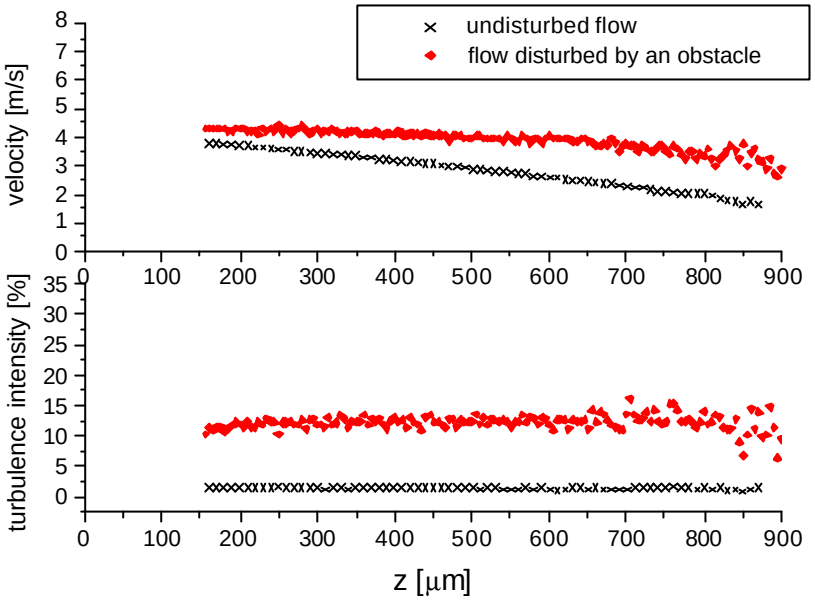

Fig.12: Comparison of the velocity profile measured in an undisturbed flow an disturbed flow (top: mean velocity, bottom: turbulence intensity).

5. DISCUSSION

The advantage of the profile sensor compared to a conventional LDA is its much higher spatial resolution because of the determination of the position of the tracer particle inside the measurement volume. The sensor does not need to be mechanically traversed for hundreds of times to obtain a velocity profile. The results of the profile sensor show the sensor has spatial resolution of several microns a measurement volume length of 750 µm, which corresponds to two order of magnitudes higher spatial resolution compared to a conventional LDA.

The present profile sensor has a spatial resolution in the micrometer range comparable to the micro-PIV/PTV techniques. An improvement down to the nanometre scale can be expected. The spatial resolution of micro-PIV /PTV techniques is determined by the aperture of the lens used for the experiment [Meinhart and Wereley 2003]. This is due to the diffraction, which is inherent in an imaging technique. However the profile sensor is not based on imaging technique, the spatial resolution is not limited by diffraction. Therefore the profile sensor has potentially higher spatial resolution compared to the micro-PIV/PTV techniques. Another advantage of the profile sensor is its long working distance. Micro-PIV/PTV technique requires small working distance with a few millimetres to obtain high spatial resolution. In contrast, the profile sensor has a working distance of several hundreds of millimetres. The present profile sensor has the working distance of 300 mm. For most of flow application the sensor should have the long working distance more than several hundreds millimetres. The long working distance of the profile sensor makes easier to be applied to flow measurements.

The temporal resolution of the LDA velocity profile sensor is important for being applied to the spectral analysis of turbulent flows. The sensor needs high temporal resolution up to several kHz of data acquisition. The present sensor has the data rate of typically around 10 Hz. The main limitation of increasing the data rate is due to the validation of signals and to the time required for processing each burst signal. Validation steps are necessary to avoid outlier data caused by inappropriate scattering signals. Until the processing finishes for a burst signal, the system has a waiting time. The present set-up utilises a standard A/D converter card and LabVIEW graphical programming which allows a quick change of the measurement program. The evaluation time can significantly

increased by using Digital Signal Processors (DSP) or Field Programmable Gate Arrays (FPGA) for data acquisition and a faster software platform (e.g. C/C++).

In the present study the measured minimum velocity was about 3 m/s (Fig. 8) due to the limitation of the signal processing technique, whose lowest measurable frequency is restricted by the pedestal of the Doppler burst signal. For the application of the velocity profile sensor for boundary layer measurement close to the wall or small velocity in a microfluidics channels, the sensor has to be able to measure low velocity down to zero. In order to realise the flow measurement with low velocity close to zero, heterodyne technique can be used. It can be realised by using two acousto-optic modulators, which are operated in different frequencies, or the quadrature demodulation technique [Müller et al. 1999].

6. CONCLUSION

A velocity profile sensor was demonstrated which allows the instantaneous determination of velocity and position of a single tracer particle passing through the measurement volume. The sensor is based on a two-wavelength technique which generates two overlapping interference fringe systems, one with converging and the other with diverging fringes. The evaluation of the ratio of the Doppler frequencies obtained from each fringe systems allows to determine the position inside the fringe systems.

The spatial resolution of the sensor was investigated experimentally and the sensor has a spatial resolution of about 1 µm within measurement volume of 750 µm at a working distance of 300 mm.

Free stream measurements were conducted in wind tunnels. Turbulence intensity of free stream was measured in an Eiffel-type wind tunnel.
Laminar and turbulent boundary layer measurements were conducted in a Göttingen-type wind tunnel. The measurement results agree well with the hot-wire measurement results obtained in the same measurement condition. The flow measurement of the wall shear stress showed excellent agreements to the Blasius theory.

The sensor offers the potential for many applications on the field of micro- and nanofluidics as well as turbulent flow research with high spatial resolution down to the Kolmogorov microscale [Tennekes and Lumley 1972].

REFERENCES

H. Albrecht, M. Borys, N. Damaschke and C. Tropea (2002) Laser Doppler and phase Doppler measurement techniques, *Springer (Heidelberg)*.

L. Büttner and J. Czarske (2001) Multimode-fiber laser-Doppler anemometer for spatially high-resolved velocity measurements using low coherent light, *Meas. Sci. Technol.*, vol.12, pp.1891-1903.

L. Büttner and J. Czarske (2003) Spatial resolving laser Doppler velocity profile sensor using slightly tilted fringe systems and phase evaluation, *Meas. Sci. Technol.*, vol.14, pp.2111-2120

L. Büttner (2004) "Untersuchung neuartiger Laser-Doppler-Verfahren zur hochauflösenden Geschwindigkeitsmessung", (in German), Dissertation, ISBN 3-86537-074-8, Cuvillier Verlag Göttingen 2003

J. Czarske (2001) Laser Doppler velocity profile sensor using a chromatic coding, *Meas. Sci. Technol.*, vol.12, pp.52-57.

J. Czarske (2001) Statistical frequency measuring error of the quadrature demodulation technique for noisy single-tone pulse signals, *Meas. Sci. Technol.*, vol.12, pp.597-614.

J. Czarske, L. Büttner, T. Razik and H. Müller, (2002) "Boundary layer velocity measurements by a laser Doppler profile sensor with micrometre spatial resolution", *Meas. Sci. Technol.* vol.13, pp.1979-1989.

F. Durst, M. Fischer, J. Jovanovic and H. Kikura (1998) Methods to set up and investigate low Reynolds number, fully developed turbulent channel flows, *J. Fluids Eng.*, vol.120, pp.496-503.

F. Durst, H. Kikura, I. Lekakis, J. Jovanovic and Q. Ye (1996) Wall shear stress determination from near-wall mean velocity data in turbulent pipe and channel flows *Exp. Fluids*, vol.20, pp.417-428.

M. Fischer, J. Jovanovic and F. Durst (2001) Reynolds number effects in the near-wall region of turbulent channel flows, *Phys. of Fluids*, vol.13, pp.1755-1767.

M. K. Mazumder, S. Wanchoo, P. C. McLeod, G. S. Ballard, S. Mozumdar and N. Caraballo (1981) Skin friction drag measurements by LDV, *Appl. Optics*, vol.20, pp.2832–2837.

C. D. Meinhart, S. T. Wereley and J. G. Santiago (1999) PIV measurements of a microchannel flow, *Exp. Fluids*, vol.27, pp.414-419.

C. D. Meinhart and H. Zhang (2000) The flow structure inside a microfabricated inkjet printhead; *J. microelectromechanical systems*, vol.9, pp.67-75.

C. D. Meinhart and S. T. Wereley (2003) The theory of diffraction-limited resolution in microparticle image velocimetry, *Meas. Sci. Technol.*, vol.14, pp.1047–1053.

P. C. Miles (1996) Geometry of the fringe field formed in the intersection of two Gaussian beams, *Appl. Optics*, vol.35, pp.5887-5895.

H. Müller, V. Strunck and D. Dopheide (1999) The application of quadrature demodulation techniques for the investigation of flows, *Flow Meas. Instrum.* vol.7, pp.237-245.

E. J. Nijhof, W. S. J. Uijttewaal and R. M. Heethaar (1993) Blood particle distributions accessed by microscopic laser-Doppler velocimetry, *Laser Anemometry Advances and Applications*, SPIE. vol.2052, pp.187-192.

Y. Sato, S. Inaba, K. Hishida and M. Maeda (2003) Spatially averaged time-resolved particle-tracking velocimetry in microspace considering Brownian motion of submicron fluorescent particles, *Exp. Fluids*, vol.35, pp.167-177.

H. Schlichting and K. Gersten (2000) Boundary layer theory (eighth edition), *Springer (Heidelberg)*.

H. Tennekes and J. L. Lumely (1972) A first course in turbulence, *MIT Press (Massachusetts)*.

A. K. Tieu, M. R. Mackenzie and E. B. Li (1995) Measurements in microscopic flow with a solid-state LDA, *Exp. in Fluids*, vol.19, pp.293-294.